

4

TECHNICAL REPORT BRL-TR-2983

BRL

AD-A206 536

COMPARISON OF COMPUTATIONAL ANALYSIS WITH FLIGHT TESTS OF A 40MM SOLID-FUEL RAMJET PROJECTILE

MICHAEL J. NUSCA
VURAL OSKAY

MARCH 1989

DTIC
SELECTED
1 APR 1989
1 APR 1989
E

APPROVED FOR PUBLIC RELEASE; DISTRIBUTION UNLIMITED.

U.S. ARMY LABORATORY COMMAND

**BALLISTIC RESEARCH LABORATORY
ABERDEEN PROVING GROUND, MARYLAND**

89 4 10 006

DESTRUCTION NOTICE

Destroy this report when it is no longer needed. DO NOT return it to the originator.

Additional copies of this report may be obtained from the National Technical Information Service, U.S. Department of Commerce, Springfield, VA 22161.

The findings of this report are not to be construed as an official Department of the Army position, unless so designated by other authorized documents.

The use of trade names or manufacturers' names in this report does not constitute indorsement of any commercial product.

REPORT DOCUMENTATION PAGE

Form Approved
OMB No. 0704-0188

1a. REPORT SECURITY CLASSIFICATION UNCLASSIFIED		1b. RESTRICTIVE MARKINGS	
2a. SECURITY CLASSIFICATION AUTHORITY		3. DISTRIBUTION / AVAILABILITY OF REPORT Approved for public release; distribution is unlimited.	
2b. DECLASSIFICATION / DOWNGRADING SCHEDULE		4. PERFORMING ORGANIZATION REPORT NUMBER(S) BRL-TR-2983	
4. PERFORMING ORGANIZATION REPORT NUMBER(S) BRL-TR-2983		5. MONITORING ORGANIZATION REPORT NUMBER(S)	
6a. NAME OF PERFORMING ORGANIZATION U.S. Army Ballistic Research Laboratory	6b. OFFICE SYMBOL (If applicable) SLCBR-LF	7a. NAME OF MONITORING ORGANIZATION	
6c. ADDRESS (City, State, and ZIP Code) Aberdeen Proving Ground, MD 21005-5066		7b. ADDRESS (City, State, and ZIP Code)	
8a. NAME OF FUNDING / SPONSORING ORGANIZATION U.S. Army Ballistic Research Laboratory	8b. OFFICE SYMBOL (If applicable) SLCBR-DD-T	9. PROCUREMENT INSTRUMENT IDENTIFICATION NUMBER	
8c. ADDRESS (City, State, and ZIP Code) Aberdeen Proving Ground, MD 21005-5066		10. SOURCE OF FUNDING NUMBERS	
		PROGRAM ELEMENT NO. 62618A	PROJECT NO. 1L1 62618AH80
		TASK NO.	WORK UNIT ACCESSION NO.
11. TITLE (Include Security Classification) Comparison of Computational Analysis with Flight Tests of a 40mm Solid-Fuel Ramjet Projectile (U)			
12. PERSONAL AUTHOR(S) Nusca, Michael J., and Oskay, Vural (NMN)			
13a. TYPE OF REPORT Technical Report	13b. TIME COVERED FROM _____ TO _____	14. DATE OF REPORT (Year, Month, Day) 1989 January	15. PAGE COUNT 35
16. SUPPLEMENTARY NOTATION			
17. COSATI CODES		18. SUBJECT TERMS (Continue on reverse if necessary and identify by block number)	
FIELD	GROUP	SUB-GROUP	
01	01		
21	08.2		
18. SUBJECT TERMS (Continue on reverse if necessary and identify by block number) Solid-Fuel Ramjet Computational Fluid Dynamics			
19. ABSTRACT (Continue on reverse if necessary and identify by block number) Flight tests of fueled and inert projectiles and a computational analysis of the non-burning internal flowfield have been used to study the performance of 40mm Solid-Fuel Ramjet (SFRJ) projectiles. These projectiles, as originally designed, did not produce detectable thrust in flight. The 40mm SFRJ is essentially scaled down from a successful 75mm round. Design modifications to the 40mm SFRJ aimed at reducing the internal velocity and/or increasing internal turbulence yielded slight performance improvements. Alternate solid fuels were found to improve thrust generation. Computational modeling is used to investigate the differences in the non-burning internal flow for 75mm and 40mm SFRJ projectiles. Analysis of internal wall pressures, shock waves and flow separation reveals that the internal flow for the 40mm geometry can be notably different from that of the 75mm geometry. These differences may have an effect on fuel ignition and burning. However, the computational analysis does not address the effects of projectile axial spin.			
20. DISTRIBUTION / AVAILABILITY OF ABSTRACT <input type="checkbox"/> UNCLASSIFIED/UNLIMITED <input checked="" type="checkbox"/> SAME AS RPT. <input type="checkbox"/> DTIC USERS		21. ABSTRACT SECURITY CLASSIFICATION UNCLASSIFIED	
22a. NAME OF RESPONSIBLE INDIVIDUAL Michael J. Nusca		22b. TELEPHONE (Include Area Code) (301)-278-2057	22c. OFFICE SYMBOL SLCBR-LF-A

Table of Contents

	<u>Page</u>
List of Figures	v
List of Tables	viii
I. Introduction	1
II. Background	2
III. 40MM Inert SFRJ Computational Results	3
1. Comparison of 40mm and 75mm SFRJ	3
2. Comparison With 40mm SFRJ Test Data	5
IV. Conclusions	7
REFERENCES	8
APPENDIX	19
DISTRIBUTION LIST	33

Accession For	
NTIS GRA&I	<input checked="" type="checkbox"/>
DTIC TAB	<input type="checkbox"/>
Unannounced	<input type="checkbox"/>
Justification	
By _____	
Distribution/	
Availability Codes	
Dist	Avail and/or Special
A-1	

List of Figures

<u>Figure</u>		<u>Page</u>
1	Geometry of the 75mm and 40mm Solid Fuel Ramjet Projectiles.	9
2	Internal Wall Pressure Distribution for the 75mm (Computed and Measured) and 40mm (Computed only) SFRJ. Wind Tunnel conditions (Mach = 4.03, Re = 20 million per foot, zero yaw). Supersonic Flow. Nozzle diameter = 1.6 in. (75mm geometry) and .853 in. (40mm geometry).	10
3	Separation Streamlines and Pressure Contours for the Internal and External Flow About the 75mm SFRJ. Wind Tunnel Conditions (Mach = 4.30, Re = 20 million per foot, zero yaw). Supersonic Flow. Nozzle diameter = 1.6 in. 11	11
4	Separation Streamlines and Pressure Contours for the Internal and External Flow About the 40mm SFRJ. Wind Tunnel Conditions (Mach = 4.30, Re = 20 million per foot, zero yaw). Supersonic Flow. Nozzle diameter = .853 in.	12
5	Internal Wall Pressure Distribution for the 75mm (Computed and Measured) and 40mm (Computed only) SFRJ. Wind Tunnel conditions (Mach = 4.03, Re = 20 million per foot, zero yaw). Subsonic Flow. Nozzle diameter = 1.1 in. (75mm geometry) and .587 in. (40mm geometry).	13
6	Pressure Contours for the Internal and External Flow About the 75mm SFRJ. Wind Tunnel conditions (Mach = 4.03, Re = 20 million per foot, zero yaw). Subsonic Flow. Nozzle diameter = 1.1 in.	14
7	Pressure Contours for the Internal and External Flow About the 40mm SFRJ. Wind Tunnel conditions (Mach = 4.03, Re = 20 million per foot, zero yaw). Subsonic Flow. Nozzle diameter = .587 in.	15
8	Pressure Contours for the Internal and External Flow About the 40mm SFRJ, Inlet region. Flight Conditions (Mach = 3.666, Re = 2 million per foot, zero yaw). Supersonic Flow. Nozzle diameter = .587 in.	16
9	Pressure Contours for the Internal and External Flow About the 40mm SFRJ, Nozzle region. Flight Conditions (Mach = 3.666, Re = 2 million per foot, zero yaw). Supersonic Flow. Nozzle diameter = .587 in.	17
10	Mosaic for Round Number 26216.	18
A1	Velocity Comparison for Inert and Modified (T-Bar in Combustor) Models - April 1985 Series	29
A2	Velocity Comparison for Non-Thrusting and 115-HVAP Fuel Models - April 1985 Series	30
A3	Velocity Comparison for Non-Thrusting and 145-HVAP Fuel Models - April 1985 Series	31

A4 Velocity Comparison for Non-Thrusting and 215-HVAP Fuel Models - April
1965 Series 32

List of Tables

<u>Table</u>		<u>Page</u>
1	COMPUTED AND MEASURED DRAG FOR ROUNDS 26219, 26220 . . .	6
2	COMPUTED DRAG BREAKDOWN FOR ROUND 26219	6
A1	MATRIX FOR OCTOBER 1984 HAWK TEST SERIES	23
A2	MATRIX FOR APRIL 1985 HAWK TEST SERIES	23
A3	MATRIX FOR MAY 1985 HAWK TEST SERIES	23
A4	MATRIX FOR DECEMBER 1984 MOSAIC TESTS	23
A5	MATRIX FOR MAY 1985 RANGE TESTS	23
A6	RESULTS FROM OCTOBER 1984 HAWK TEST SERIES	24
A7	RESULTS FROM APRIL 1985 HAWK TEST SERIES	25
A8	RESULTS FROM MAY 1985 HAWK TEST SERIES	26
A9	RESULTS FROM MAY 1985 HAWK TEST SERIES	27
A10	RESULTS FROM MAY 1985 HAWK TEST SERIES	28

I. Introduction

The auto-ignition of solid-fuel ramjet (SFRJ) projectiles has been a subject of controversy and research. During the initial development of various SFRJ projectiles of varying caliber (20mm, 40mm, and 75mm), the selection of internal geometries and fuel composition was not aided by detailed numerical simulation of the flow. This report documents 40mm flight test data and numerical simulations that could be used in the design evolution of SFRJ projectiles.

Computational modeling and wind tunnel testing of the internal and external flow for a 75mm SFRJ projectile (Figure 1) has been under way at the Ballistic Research Laboratory (BRL) Launch and Flight Division (LFD). A computational fluid dynamics (CFD) code utilizing an implicit, factored, time-stepping algorithm in a zonal grid framework has been developed by Chakravarthy.^{1,2} This code employs a class of numerical algorithms, termed total variational diminishing or TVD, which do not require the inclusion of smoothing or dissipation functions to achieve numerical stability. The code can be used in conjunction with various turbulence and separated flow modeling techniques. Modeling strategies investigated include: a) the Baldwin-Lomax turbulence model³ applied throughout the flowfield; b) the Baldwin-Lomax model applied outside of backflow regions, and the backflow turbulence model of Goldberg⁴ applied within these regions. This code has been previously employed in the solution of subsonic, transonic, supersonic and mixed flow problems including complex supersonic inlet and nozzle flows by Chakravarthy⁵

Nusca, Chakravarthy, and Goldberg⁶ have applied this code to the internal and external flow of inert 75mm SFRJ projectiles of various internal configuration (i.e. D_2 and D_3 , see Figure 1). Internal wall pressure distributions were compared with those measured in full-scale wind tunnel models⁷. The capability of the code to match the measured pressures was demonstrated. The details of the internal flowfield were analyzed for supersonic and subsonic (choked) internal flow conditions.

This computational capability has been used to analyze the internal flow in an inert 40mm SFRJ at zero yaw. The aim of this analysis is to determine the differences in internal flow patterns between the 75mm and 40mm SFRJ models. The dimensions of the 40mm model are essentially scaled from those of the 75mm (see Figure 1). The flight per-

¹ Chakravarthy, S.R. "A New Computational Capability for Ramjet Projectiles," ARBRL-CR-595, U.S. Army Ballistic Research Laboratory, Aberdeen Proving Ground, MD, March 1988.

² Goldberg, U.C., Chakravarthy, S.R., and Nusca, M.J., "A New Computational Capability for Ramjet Projectiles." AIAA-87-2411, Proceedings of the 14th AIAA Atmospheric Flight Mechanics Conference, Monterey, CA, August 17-19, 1987.

³ Baldwin, B.S. and Lomax, H., "Thin Layer Approximation and Algebraic Model for Separated Turbulent Flows." AIAA-78-257, Proceedings of the 16th AIAA Aerospace Sciences Meeting, Huntsville, AL, January 16-18, 1978.

⁴ Goldberg U.C., "Separated Flow Treatment with a New Turbulence Model," *AIAA Journal*, Vol. 24, No. 10, October 1986, pp. 1711-1719.

⁵ Chakravarthy S.R., Szema K.Y., Goldberg U.C., Gorski J.J. (Rockwell International Science Center) and Osher S. (University of California), "Application of a New Class of High Accuracy TVD Schemes to the Navier-Stokes Equations." AIAA-85-0165, Proceedings of the 23rd AIAA Aerospace Sciences Meeting, Reno NV., January 14-17, 1985.

⁶ Nusca, M.J., Chakravarthy, S.R., and Goldberg, U.C., "Computational Fluid Dynamics Capability For The Solid Fuel Ramjet Projectile," ARBRL-TR-2958, U.S. Army Ballistic Research Laboratory, Aberdeen Proving Ground, MD, December 1988.

⁷ Kayser, L.D., Yalamanchili, R.J., Trezler, C., "Pressure Measurements on the Interior Surface of a 75mm Tubular Projectile at Mach 4," US Army Ballistic Research Laboratory, Aberdeen Proving Ground, MD, report in preparation.

formance of the 75mm rounds, documented previously,^{8,9} is superior to the 40mm round documented herein. The computed leading edge and base flowfields for the 40mm SFRJ are compared with photographs of inert rounds at essentially zero yaw. The computed and measured drag coefficients are also compared.

II. Background

During the early 1980's, U.S. Army Chemical Research Development and Engineering Center (CRDEC) began development of a 40mm Solid-Fuel Ramjet (SFRJ) projectile as a possible air defense round. This concept was an extension of the CRDEC Tubular Projectile (TUP) development program. By means of internally contained solid fuel, the proposed tubular projectile was designed to have an elevated velocity (or at least a constant one) for 4000m of range. Before 1984, CRDEC had already attempted several design modifications. However, none of the rounds produced thrust as defined by detectable changes in velocity histories. At that time, both CRDEC and United Technologies Chemical Systems Division (UTC-CSD), the manufacturer of the 40mm SFRJ, decided that the reason for the poor performance of these rounds was that the internal flow was supersonic and that subsonic internal flow was required for combustion.

In October 1984, a series of tests were conducted with modified projectiles that contained internal devices designed to reduce internal velocity and/or increase flow turbulence. All modified configurations showed some drag reduction compared to unmodified, non-burning versions. However, two issues concerning the flight performance of the round remained to be investigated: (a) the location of the inlet shock and (b) the effects of projectile axial spin on the solid fuel performance. The question of shock location was resolved via testing. Three rounds were fired in the BRL-LFD Transonic Range (TR),¹⁰ to obtain photographic data on the shock location.

A series of tests were designed to determine the possibility of improved flight performance for the 40mm SFRJ by changing the fuel composition. An original fuel composition (406 HVAP, Heat of VAPorization) was replaced, for this series, by more-energetic fuel compositions (215-HVAP UTF 25950, 145-HVAP UTF 25048, and 115-HVAP UTF 22032). UTF 22032 is the same fuel composition used in the 75mm TGTR (Tank Gun Training Round).⁹

In May 1985, 215-HVAP fuel was tested for consistent performance. All rounds showed reduced drag. However, the observed break points in the velocity curves, where transition to the non-thrusting mode occurred, were not consistent.

A brief chronology of the 40mm SFRJ test firing programs along with descriptions of firing test setup, and some results, in the form of velocity-time plots, are given in the Appendix.

⁸ Mermagen, W.H., and Yalamanchili, R.J., "First Diagnostic Tests of a 75mm Solid Fuel Ramjet Tubular Projectile," ARBRL-MR-03283, US Army Ballistic Research Laboratory, Aberdeen Proving Ground, MD, June 1983. (AD A130598)

⁹ Mermagen, W.H., and Yalamanchili, R.J., "Experimental Tests of a 105/75 mm Solid Fuel Ramjet Tubular Projectile," ARBRL-MR-3416, US Army Ballistic Research Laboratory, Aberdeen Proving Ground, MD, December 1984. (AD B089766)

¹⁰ Rogers, W.K., Jr., "The Transonic Free Flight Range", Ballistic Research Laboratory Report No. 1044, US Army Ballistic Research Laboratory, Aberdeen Proving Ground, MD, June 1958. (AD 200177)

III. 40MM Inert SFRJ Computational Results

The computational fluid dynamics (CFD) approach described in Reference 6 can be used to predict the compressible flowfield in and around an aerodynamic projectile by solving the 2D or 3D Navier-Stokes equations. At present only axisymmetric (zero yaw) flows have been investigated. These equations are solved with the assumption that the flow medium is air behaving as a perfect gas and that no chemical reactions are occurring. As a result only inert SFRJ projectiles are addressed at present. These equations are transformed into conservation law form and discretized using finite volume approximations and the TVD formulation. The resulting set of equations are solved using an implicit, factored, time-stepping algorithm. This solution takes place on a computational grid that is generated around the projectile in zones, the zonal boundaries of which can be made transparent to the flowfield solution.

The internal flowfield of the SFRJ projectile includes large regions of recirculating flow. These separated flow regions are induced by sharp geometrical discontinuities such as the injector and nozzle entrance (see Figure 1). Indeed, internal surface pressure measurements made on an instrumented 75mm SFRJ wind tunnel model (unfueled) indicate that such regions do exist in the inlet and combustion sections.⁷ Accurate modeling of these regions is critical to the accuracy of the overall flowfield solution. Goldberg⁴ has developed a turbulence/backflow model based on experimental observations of separated turbulent flows. This model has been used to successfully compute the internal flow for a 75mm SFRJ.⁶ As discussed in Reference 6, the accurate location of the flow transition point (from laminar to turbulent flow) is critical to achieving agreement between measured and computed internal wall pressures. Thus, the transition point was chosen based on measured data.

1. Comparison of 40mm and 75mm SFRJ

The computational solutions have been compared with the internal surface pressure measurements on an inert 75mm SFRJ model. The model was instrumented with pressure taps and mounted in the Mach 4, nine-inch blowdown tunnel at the NASA Langley Research Center. The details of these tests are described in Reference 7. The freestream Mach number and Reynolds number were 4.03 and about 20 million per foot, respectively. The model was at zero yaw.

Figure 2 shows the internal wall pressure distribution for the 75mm SFRJ, both computed and measured, and the 40mm SFRJ, computed only. The injector and nozzle diameters (D_2 and D_3) for the 75mm model are 1.7 inches and 1.6 inches, respectively. For the 40mm model an injector diameter of .873 inches and a nozzle diameter of .825 inches were used. The agreement between measured and computed pressure distributions, for the 75mm model, is good. The constant pressure in the inlet ($0 \leq x < 3$) is due to a separation bubble that extends from the leading edge to the injector. A pressure rise is observed over the injector step. Through the combustion section ($3 < x < 9$), a pressure gradient is caused by a separation bubble that increases in thickness from the injector to the nozzle. Thus, the flow through the core of the SFRJ is constricted at the nozzle entrance to a larger degree

than at the injector. Flow expansion is achieved through the nozzle. Thus, the 75mm SFRJ non-reacting flow is characterized by flow separation that dominates the inlet and the combustion sections.

The 40mm SFRJ is essentially a scaled-down version of the 75mm SFRJ in that the diameters (inlet, injector, nozzle, nozzle exit) are approximately the same as the ratio of the maximum diameters, 40/75 (see Figure 1). The lengths of the model components, as well as the overall length, are not scaled. Relative to the 75mm model, the overall length of the 40mm model and the lengths of the component parts are smaller than those of the 75mm model.

The pressure distribution for the 40mm SFRJ flight configuration (Figure 2) indicates a very different internal flowfield, relative to the 75mm model. Thru the inlet ($0 \leq x \leq 1.3$), the flow is similar to that of the 75mm model, constant pressure and separated flow over the entire length. However, in the combustion section ($1.3 < x \leq 5.9$), the flow is not dominated by separation, as is the case for the 75mm model. The flow separates behind the injector and forms a recirculation bubble, but reattaches on the horizontal wall and remains attached over most of the section. This is indicated by the near constant pressure thru most of the combustion section. Near the forward-facing step that precedes the nozzle (see Figure 1), the flow again separates and forms a bubble of recirculating flow. This bubble causes a sharp pressure rise at about $x = 5$ inches, before the nozzle.

Computed results for inert 75mm and 40mm SFRJ models show that the internal flow of the 40mm model is unique. The basic flow differences discussed above are also seen in the separation streamlines and pressure contours of Figures 3 and 4. Both the 75mm and the 40mm models show an attached leading edge shock wave and a shock that is generated by the injector. These shocks intersect normal to the centerline and reflect. Both inlets are dominated by separated flow. In the 75mm model, the pressure gradient normal to the wall in the combustion section is constant, indicating a separated flow region. This is confirmed by a separation streamline that connects the injector and nozzle. In the 40mm model, the pressure gradient normal to the wall in the combustion section is constant for a small distance behind the injector and in front of the nozzle. This indicates two small separated flow regions with attached flow thru most of the combustion section. This is confirmed by a separation streamline behind the injector and before the nozzle entrance. The separation bubble in front of the nozzle generates a shock that intersects normal to the centerline. Thus the 75mm and 40mm SFRJ projectiles constitute two very different internal flowfields due mainly to flow separation.

Figure 5 shows the internal wall pressure distribution for the 75mm SFRJ, both computed and measured, and the 40mm SFRJ, computed only. The injector and nozzle diameters (D_2 and D_3) for the 75mm model are 1.7 inches and 1.1 inches, respectively. For the 40mm model an injector diameter of .873 inches and a nozzle diameter of .587 inches were used. Since these diameters are not used in the flight vehicle, this calculation serves only as an additional comparison on the flowfields. The agreement between measured and computed pressure distributions, for the 75mm model, is good. The higher pressure level for these smaller nozzle diameters indicates subsonic internal flow caused by an expelled leading edge normal shock. In this case the pressure distribution for the 40mm model is similar to that of the 75mm model, however the pressure level is slightly reduced.

Figures 6 and 7 show the pressure contours for the 75mm and 40mm SFRJ models, respectively. In both cases a normal shock is clearly seen at the leading edge. Upon detailed examination, the presence of flow spillage to the exterior has been found. The subsonic interior flow expands through the diverging inlet, and the pressure remains relatively constant throughout the combustion section. Expansion back to supersonic flow is accomplished by the nozzle.

Thus, for large nozzle diameters (flight vehicle configuration) and supersonic internal flow, the non-burning internal flowfield for the 75mm and 40mm SFRJ models are dissimilar (as indicated by internal wall pressure distributions and contours). For the smaller nozzle diameters and subsonic internal flow, these flowfields are similar with slightly different internal wall pressures. Although these results are for the non-reacting flows, they serve as a basis for the proposition that fueled 75mm and 40mm SFRJ projectiles may perform dissimilarly in flight. This proposition is consistent with flight data.

2. Comparison With 40mm SFRJ Test Data

Computed results for the 40mm SFRJ subject to flight conditions have been performed. Since the present computations are for zero yaw, rounds with small average yaw - Round Nos. 26219 ($\alpha = 1.74$ degs.) and 26220 ($\alpha = 1.77$ degs.), (Table A8) - are analyzed for zero yaw. The flight Mach numbers are 3.678 and 3.666, respectively, and the Reynolds numbers are about 1.7 million per foot. The basis for comparison with flight tests is a mosaic picture of round 26216 showing the leading edge and nozzle exit flowfields, and drag coefficients as determined from Transonic Range measurements.

Figure 8 and 9 show the computed pressure contours for round 26220 in the vicinity of the inlet and the nozzle, respectively. In order to display the most detail, these figures have different scales. Figure 8 shows that the leading edge shock wave is attached to the inlet. The exterior shockwave angle is approximately 30 degrees. The mosaic for this round (Figure 10) shows the attached exterior shock from a side view, thus the blurring seen at the leading edge. The computed flow picture is in good agreement with this mosaic. The computed interior shockwave angle is approximately 20 degrees and intersects normal to the centerline at about .8 inches from the leading edge. Figure 9 shows the flowfield aft of the nozzle. The flow that is exiting the nozzle is supersonic (Mach number 2.7). A highly curved oblique shock wave is generated near the base of the projectile. This shock intersects normal to the centerline (in a Mach disk) at about 2.3 inches from the base. The flow along the centerline from the nozzle exit to the Mach disk is accelerated from Mach 2.7 to 5.8. At the Mach disk the flow Mach number is reduced to 1.6. The mosaic (Figure 10) confirms the highly curved oblique shock from the base of the projectile. The observed shock intersects normal to the centerline at about 1.4 inches from the base (the mosaic image is a 20% enlargement). The source of the discrepancy between computed and measured Mach disk location may be due in part to a turbulence generation device (screen) inside the ramjet. The presence of this device is not accounted for in the computation and mosaics for rounds without the device (No. 26219 or 26220) are not available.

The in-flight aerodynamic drag of several inert SFRJ rounds has been obtained by range measurements (see Table A10). Round numbers 26219 and 26220 were of the stan-

standard 40mm SFRJ design. Drag data for these rounds were obtained for Mach numbers around 3.66 and for yaw angles smaller than 1.8 degs. The computations for these rounds are for zero yaw. Computed and measured drag coefficient are compared in Table 1. Differences in computed and fitted zero-yaw drag coefficient are between 8 and 14%. These differences are caused by inaccuracies in the computation. Comparison between computed and measured internal wall pressures for the 75mm configuration showed that the computation underpredicts the pressure. Assuming that the same is true for the 40mm configuration, these wall pressure differences result in a difference in drag coefficient of about 4%. Inaccuracies in the computation of internal wall skin friction, especially in the backflow regions, could also significantly effect the computed drag since this component accounts for about 20% of the total drag (see Table 2).

Table 1. COMPUTED AND MEASURED DRAG FOR ROUNDS 26219, 26220

	Round No. 26219		Round No. 26220	
	Drag Coeff.	% of Total	Drag Coeff.	% of Total
Inlet	.010	4.4	.010	4.4
Total Interior (incl. Inlet)	.115	50.9	.116	50.9
Total Exterior	.111	49.1	.112	49.1
Total Drag	.226		.228	
Measured Range Total Drag	.285		.290	
Fitted Zero-Yaw Total Drag	.245		.265	
Round No. 26219, Mach No. = 3.678, Yaw Angle = 1.74 degs.				
Round No. 26220, Mach No. = 3.666, Yaw Angle = 1.77 degs.				

For a typical round, computed drag data reveal that the pressure drag from the external and internal surfaces and the wall friction drag from the internal surface are the largest contributors to the total drag. Table 2 provides the breakdown in these contributions. The large contribution from interior wall friction drag is caused by regions of separated flow. In contrast, the attached flow over the exterior surface yields a low wall friction drag value. Since the injector and nozzle entrance are oriented normal to the incoming flow, the drag contribution from these surfaces are large. The small contribution from the base drag is due to the small base area and is typical for nozzle wake flows.

Table 2. COMPUTED DRAG BREAKDOWN FOR ROUND 26219

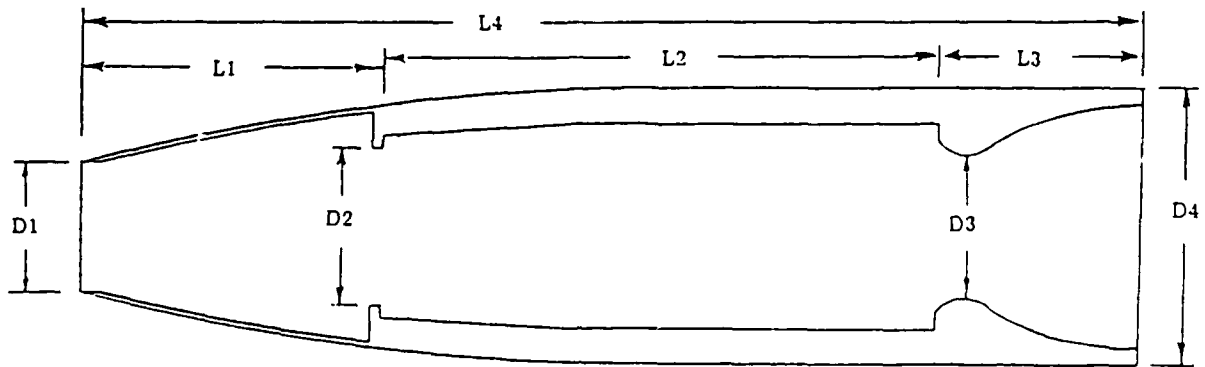
Drag Contribution	% of total
Exterior pressure drag	37.3
Interior wall friction drag	19.4
Interior pressure drag (injector and nozzle entrance)	18.0
Interior pressure drag (all other surfaces)	13.4
Base drag	6.3
Exterior wall friction drag	5.6

IV. Conclusions

Flight tests of fueled and inert ramjet projectiles, and computational analysis of the non-burning internal flowfield have been used to study the performance of 40mm Solid Fuel Ramjet (SFRJ) rounds. These rounds, as originally designed, did not produce detectable thrust in flight. The 40mm SFRJ round is essentially scaled from the 75mm round. Successful flight testing of the 75mm round has been previously documented. Design modifications to reduce internal velocity and/or increase internal turbulence yielded slight performance improvements. Alternate solid fuels were found to improve thrust generation. Computational modeling of the non-burning internal flow in 75mm and 40mm SFRJ projectiles are compared. Analysis of internal wall pressures, shock waves and flow separation reveals that the internal flow of the 40mm geometry is notably different from that of the 75mm geometry for supersonic internal flow conditions. For subsonic internal flow conditions the 40mm geometry produces a similar trend in wall pressure, but these pressures are slightly smaller than those computed for the 75mm round. Although these results are for the non-reacting flows, they serve as a basis for the proposition that fueled 75mm and 40mm SFRJ projectiles may perform dissimilarly in flight. This proposition is consistent with flight data.

References

1. Chakravarthy S.R. "A New Computational Capability for Ramjet Projectiles," ARBRL-CR-593, U.S. Army Ballistic Research Laboratory, Aberdeen Proving Ground, MD, May 1988.
2. Goldberg, U.C., Chakravarthy, S.R., and Nusca, M.J. "A New Computational Capability for Ramjet Projectiles," AIAA-87-2411, Proceedings of the 14th AIAA Atmospheric Flight Mechanics Conference, Monterrey, CA, August 17-19, 1987.
3. Baldwin, B.S. and Lomax, H., "Thin Layer Approximation and Algebraic Model for Separated Turbulent Flows," AIAA Paper No. 78-257, January 1978.
4. Goldberg U.C., "Separated Flow Treatment with a New Turbulence Model," AIAA Journal, Vol. 24, No. 10, October 1986, pp. 1711-1713.
5. Chakravarthy S.R., Szema K.Y., Goldberg U.C., Gorski J.J. (Rockwell International Science Center) and Osher S. (University of California), "Application of a New Class of High Accuracy TVD Schemes to the Navier-Stokes Equations," AIAA-85-0165, Proceedings of the 23rd AIAA Aerospace Sciences Meeting, Reno NV., January 14-17, 1985.
6. Nusca, M.J., Chakravarthy, S.R., and Goldberg, U.C., "Computational Fluid Dynamics Capability For The Solid Fuel Ramjet Projectile," ARBRL-TR-2958, U.S. Army Ballistic Research Laboratory, Aberdeen Proving Ground, MD, December 1988.
7. Kayser, L.D., Yalamanchili, R.J., Trexler, C., "Pressure Measurements on the Interior Surface of a 75mm Tubular Projectile at Mach 4," US Army Ballistic Research Laboratory, Aberdeen Proving Ground, MD, report in preparation.
8. Mermagen, W.H., and Yalamanchili, R.J., "First Diagnostic Tests of a 75mm Solid Fuel Ramjet Tubular Projectile," ARBRL-MR-03283, US Army Ballistic Research Laboratory, Aberdeen Proving Ground, MD, June 1983. (AD A130598)
9. Mermagen, W.H., and Yalamanchili, R.J., "Experimental Tests of a 105/75 mm Solid Fuel Ramjet Tubular Projectile," ARBRL-MR-3416, US Army Ballistic Research Laboratory, Aberdeen Proving Ground, MD, December 1984. (AD B089766)
10. Rogers, W.K., Jr., "The Transonic Free Flight Range", Ballistic Research Laboratories Report No. 1044, US Army Ballistic Research Laboratory, Aberdeen Proving Ground, MD, June 1958. (AD 200177)



	75mm Geometry	40mm Geometry
D1	1.40	0.801
D2	1.70	0.873
D3	1.60	0.853
D4	2.95	1.574
L1	3.00	1.319
L2	5.54	4.500
L3	2.00	3.792
L4	10.54	6.619
All dimensions in inches		

Figure 1. Geometry of the 75mm and 40mm Solid Fuel Ramjet Projectiles.

Navier-Stokes Computation for SFRJ 75mm and 40mm Configurations

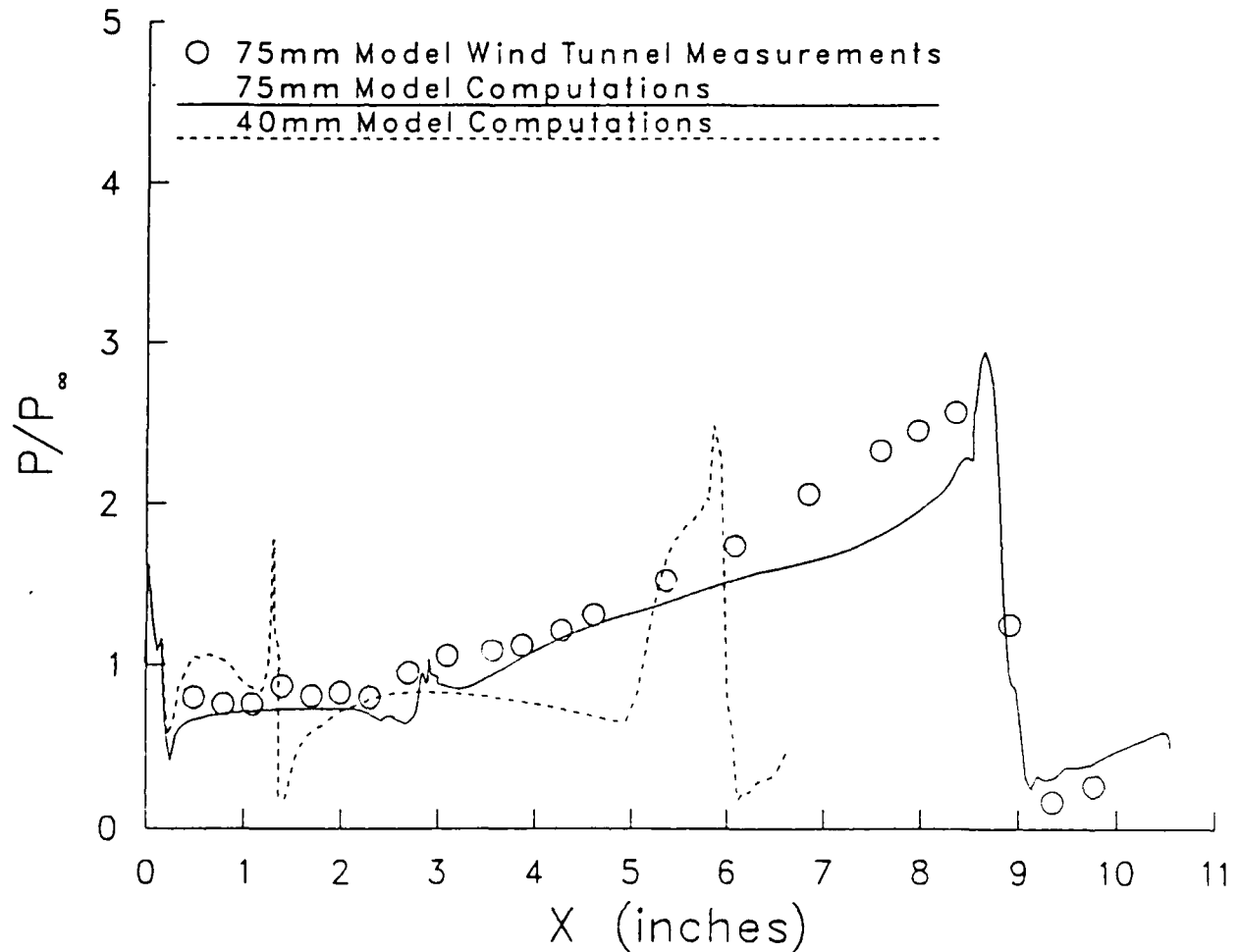


Figure 2. Internal Wall Pressure Distribution for the 75mm (Computed and Measured) and 40mm (Computed only) SFRJ. Wind Tunnel conditions (Mach = 4.03, Re = 20 million per foot, zero yaw). Supersonic Flow. Nozzle diameter = 1.6 in. (75mm geometry) and .853 in. (40mm geometry).

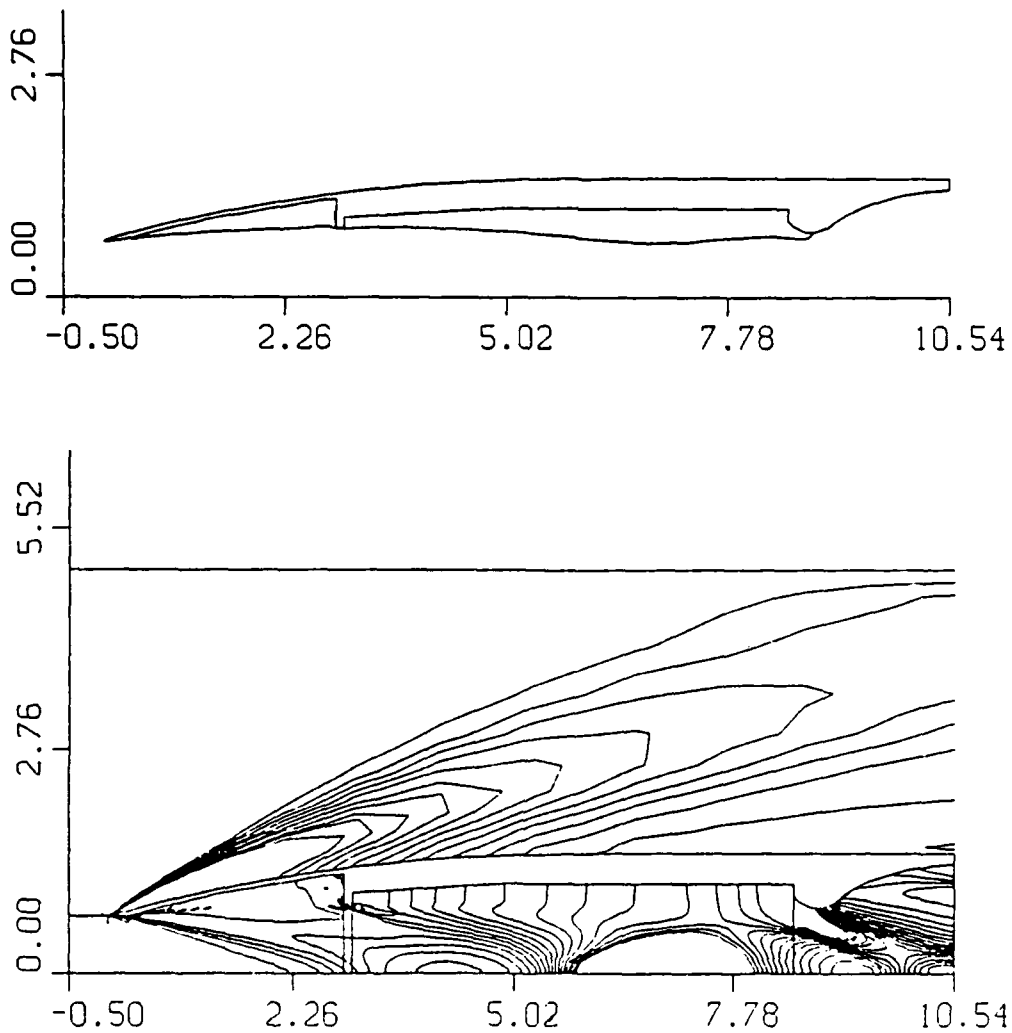


Figure 3. Separation Streamlines and Pressure Contours for the Internal and External Flow About the 75mm SFRJ. Wind Tunnel Conditions (Mach = 4.30, Re = 20 million per foot, zero yaw). Supersonic Flow. Nozzle diameter = 1.6 in.

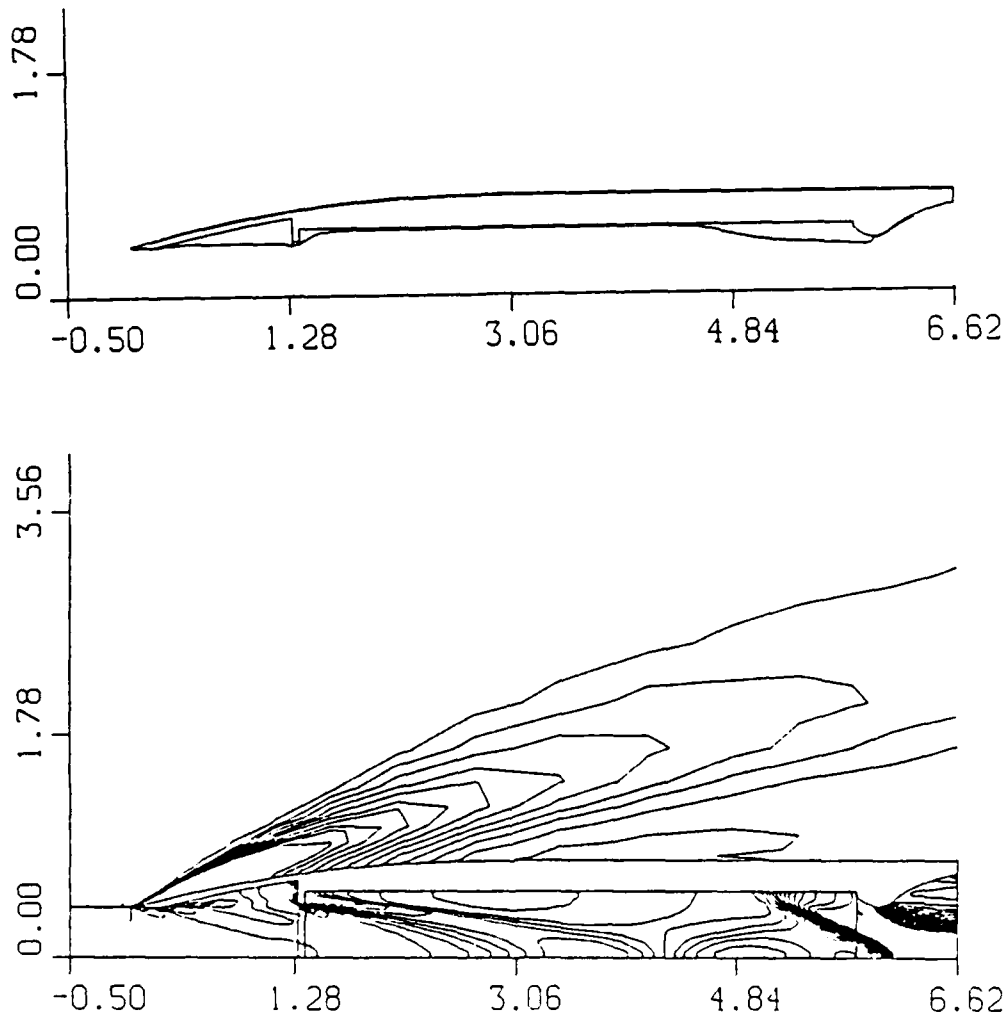


Figure 4. Separation Streamlines and Pressure Contours for the Internal and External Flow About the 40mm SFRJ. Wind Tunnel Conditions (Mach = 4.30, Re = 20 million per foot, zero yaw). Supersonic Flow. Nozzle diameter = .853 in.

Navier-Stokes Computation for SFRJ 75mm and 40mm Configurations

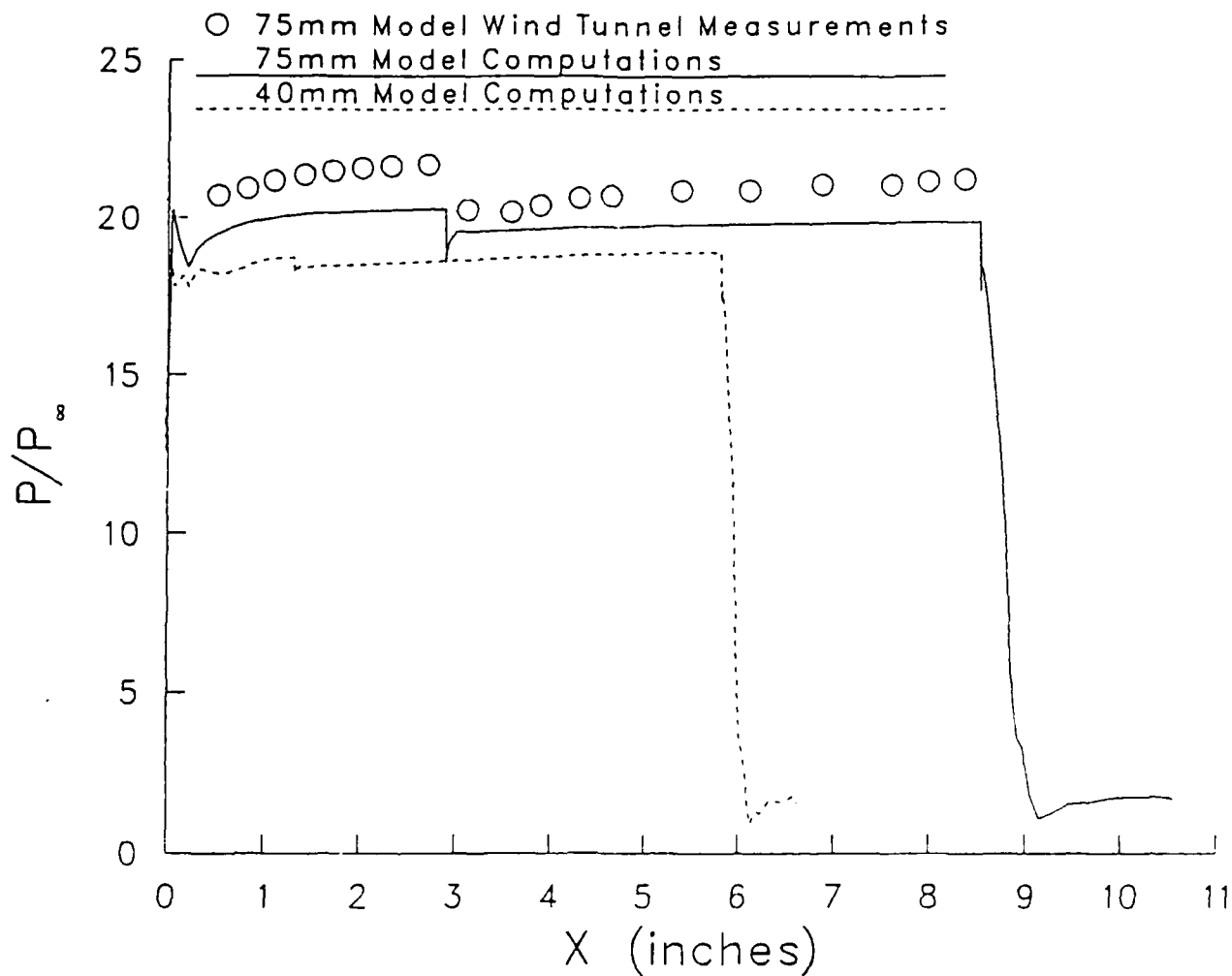


Figure 5. Internal Wall Pressure Distribution for the 75mm (Computed and Measured) and 40mm (Computed only) SFRJ. Wind Tunnel conditions (Mach = 4.03. Re = 20 million per foot, zero yaw). Subsonic Flow. Nozzle diameter = 1.1 in. (75mm geometry) and .587 in. (40mm geometry).

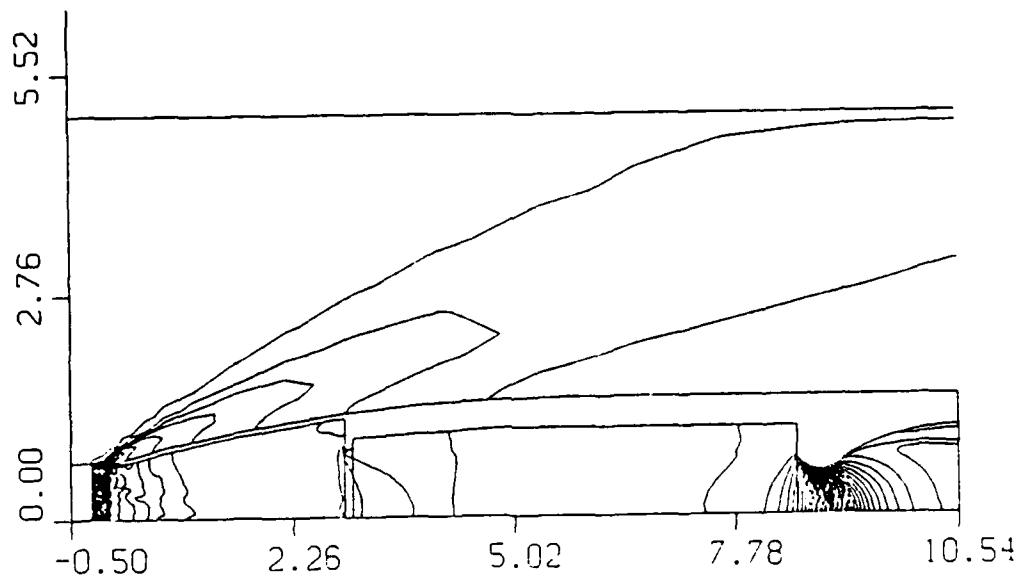


Figure 6. Pressure Contours for the Internal and External Flow About the 75mm SFRJ. Wind Tunnel conditions (Mach = 4.03, Re = 20 million per foot, zero yaw). Subsonic Flow. Nozzle diameter = 1.1 in.

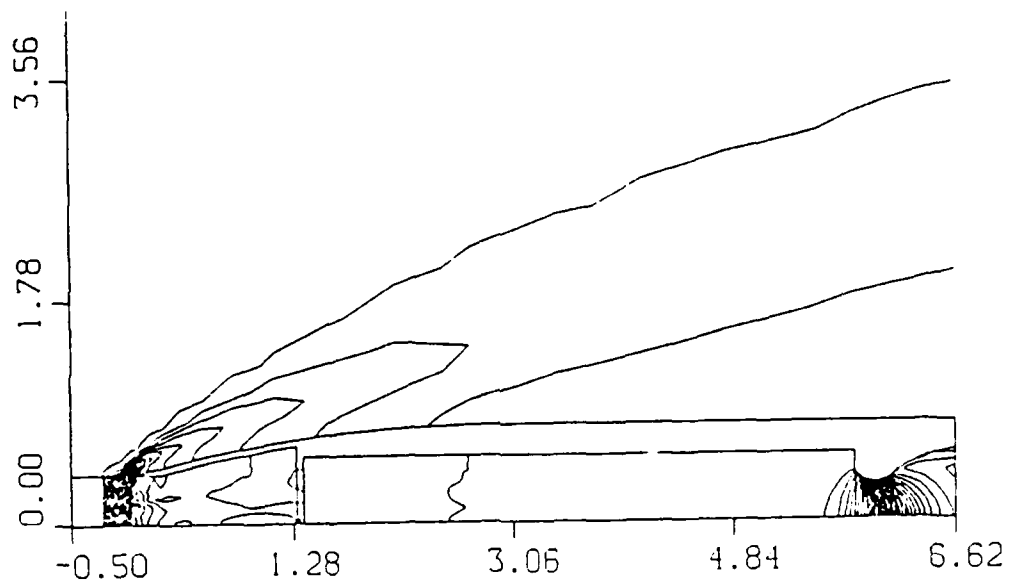


Figure 7. Pressure Contours for the Internal and External Flow About the 40mm SFRJ. Wind Tunnel conditions (Mach = 4.03, Re = 20 million per foot, zero yaw). Subsonic Flow. Nozzle diameter = .587 in.

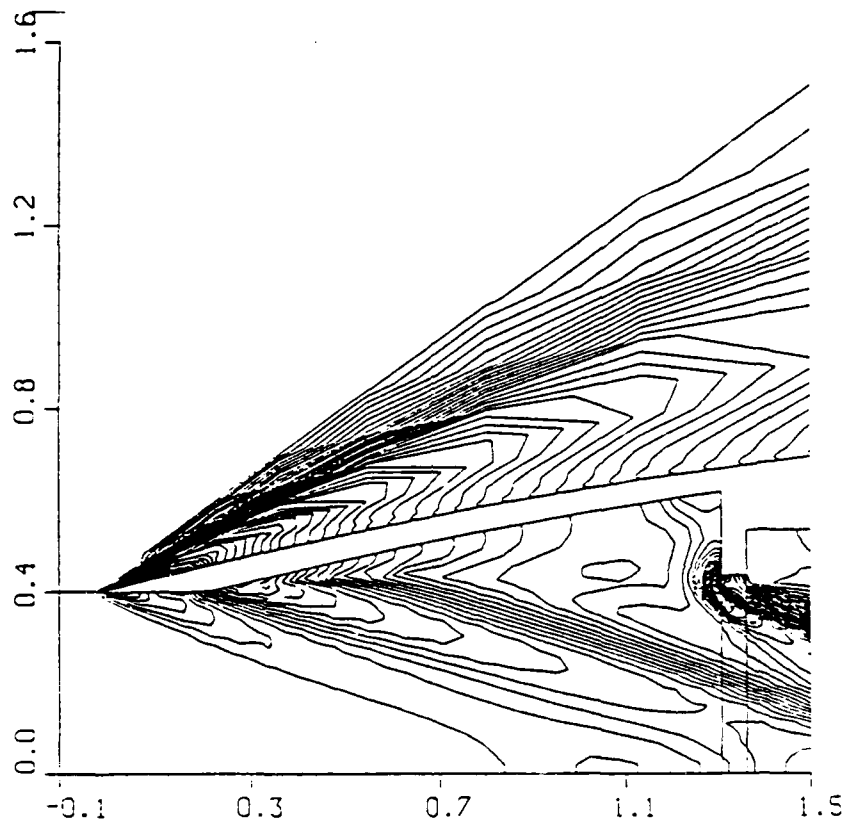


Figure 8. Pressure Contours for the Internal and External Flow About the 40mm SFRJ, Inlet region. Flight Conditions (Mach = 3.666, Re = 2 million per foot, zero yaw). Supersonic Flow. Nozzle diameter = .587 in.

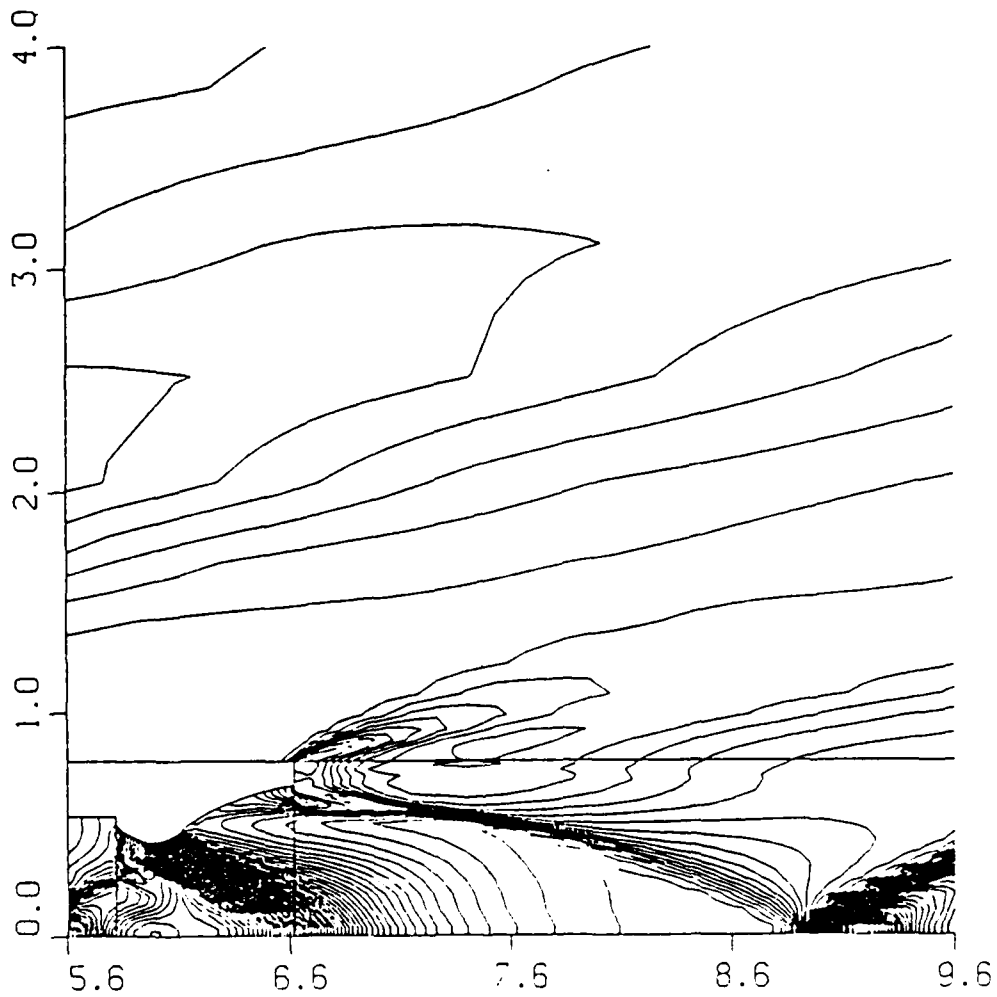


Figure 9. Pressure Contours for the Internal and External Flow About the 40mm SFRJ. Nozzle region. Flight Conditions (Mach = 3.666, Re = 2 million per foot, zero yaw). Supersonic Flow. Nozzle diameter = .587 in.

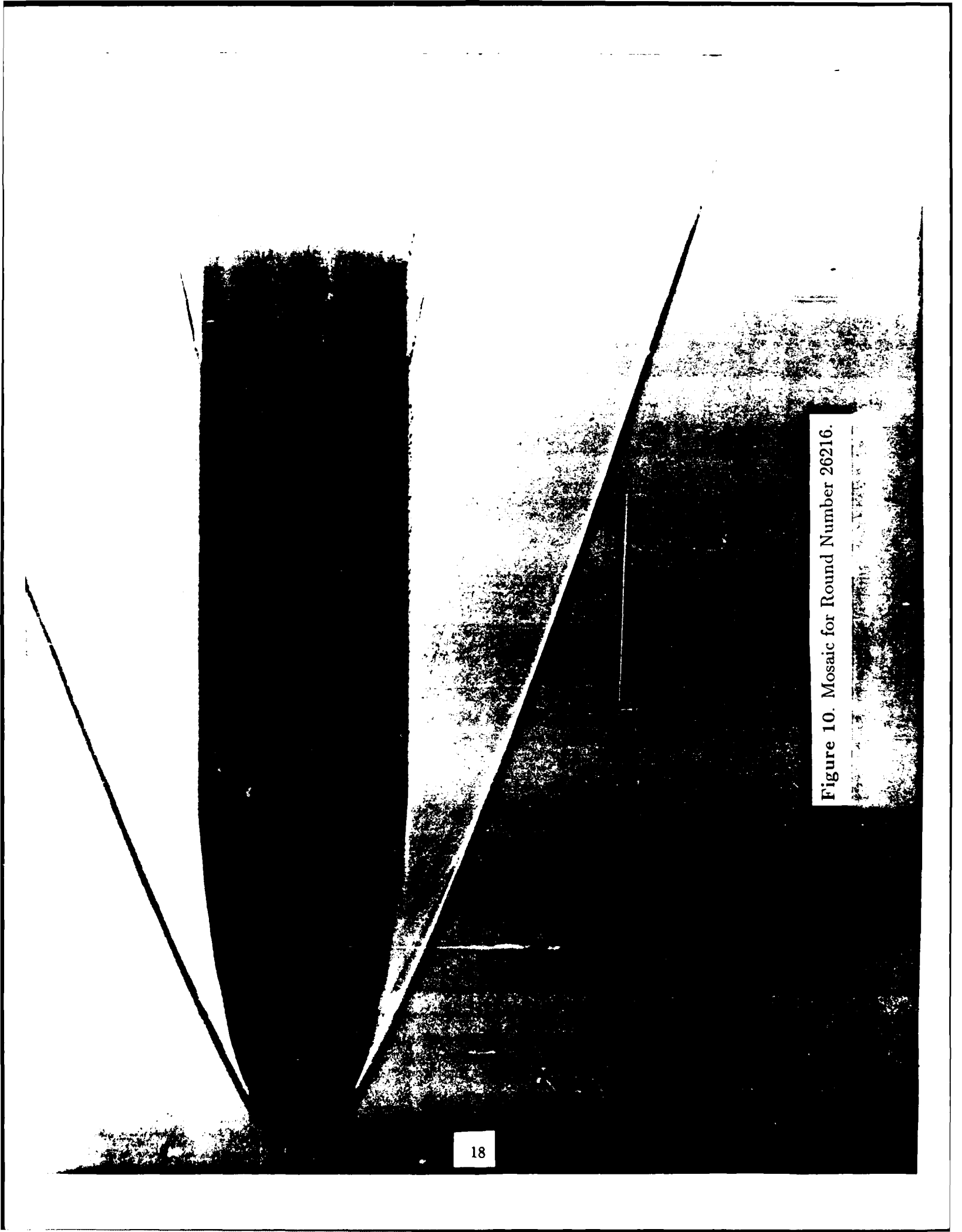


Figure 10. Mosaic for Round Number 26216.

APPENDIX

40MM SFRJ Test Chronology

Two types of test programs were conducted for the 40mm SFRJ models. One type of test involved tracking the round with a Hawk doppler radar during flight and determining projectile velocity history. These tests are described as "Hawk Tests". The second type of test was done in the Transonic Range (TR) facility to collect photographic data to determine aerodynamic coefficients. These tests are designated "Range Tests". Test matrices and the instrumentation requirements are discussed separately in the following sections.

Hawk Tests

The Hawk Tests were used to observe the velocity history of the 40mm SFRJ rounds in flight. The main instrumentation consisted of a Hawk doppler radar. The output of the Hawk radar is an analog frequency that is proportional to the projectile's slant velocity. This signal can be reduced to a velocity history as a function of flight time through the use of a radar constant. The Hawk radar was supplemented with 35mm smear cameras to observe sabot separation and metal parts integrity and to record visible hot gases in the wake of the SFRJ projectile.

The October 1984 test series was conducted to determine if internal design modifications could improve the performance of the 40mm SFRJ. The program, consisting of ten rounds, yielded velocity histories from the Hawk doppler radar. Table A1 is the test matrix for this series.

A test series with Hawk support was also fired during April 1985. The purpose of this program was to determine the performance variations of the 40mm SFRJ using fuels of different combustion intensity. The test matrix is shown in Table A2.

A test series with Hawk support fired in May 1985 was used to determine consistent performance of the 215 HVAP (Heat of VAPorization) fuel in the 40mm SFRJ. The test matrix for this series is shown in Table A3.

Range Tests

Two sets of Range Tests were conducted. The purpose of the first series was to determine the inlet shock location for the 40mm SFRJ. Therefore, the main emphasis was on mosaic photography. The second set of tests were fired to obtain aerodynamic data for the SFRJ in addition to the mosaic data.

The basic TR instrumentation consists of 25 orthogonal shadowgraph stations. These stations are spaced as five groups of five stations each. Within a group, the stations are separated by 20 ft (6 m). However, the last station of one group is 70 ft (21 m) from the first station of the next group. Thus, the instrumented section of the TR is 680 ft (207 m). Each of these stations are individually surveyed with respect to a master survey system so that the spatial position of a projectile can be determined from shadowgraph pictures at the time of exposure. This time/position data and the measured angles of the projectile at each station are used to compute the aerodynamic coefficients of the test vehicle.

A mosaic station is a special setup used to directly observe the flowfield about a projectile in free flight. This station is a collage of open film sheets placed on a stand within TR. The station is triggered by the passage of the projectile, and a spark exposes the film and creates an image of the projectile flowfield. During this program, the mosaic station was set up at about 400 ft (122 m) from the gun.

The first TR test, in December 1984, was used to obtain mosaic data on the leading edge shock location for the 40mm SFRJ. This test consisted of two segments as shown in Table A4.

The first portion of the test program was to observe the separation of the projectile pusher plate in order to minimize any possibility of damage to the TR instrumentation.

The main instrumentation was three smear cameras located at 12, 30, and 60 ft (4, 9, and 18 m, respectively) from the gun, and a target located at 100 ft (30 m) to simulate the location of the TR entrance. After determining that 40mm rounds could be predictably launched, three rounds were fired through TR. Although the standard TR setup was used, the main purpose of this series was to obtain mosaic data on the inlet shock location.

The second set of TR tests were used to determine aerodynamic coefficients and mosaic data for the basic projectile (i.e., a 40mm SFRJ with inert fuel) and several modifications. The test matrix for this series is shown in Table A5.

40MM SFRJ Test Results

The results to be discussed are: "Hawk Tests" plots of velocity versus time and "Range Tests" results showing the flowfield around the projectile and aerodynamic coefficients.

Hawk Tests

The October 1984 tests were to determine if any of the physical modifications to the projectile improved the burning properties of the 406-HVAP fuel. The preliminary data from this series are shown in Table A6. For the October tests, the launch velocities ranged from 4400 to 4600 ft/sec. The velocity history for the standard design, Round 25255, showed that this round failed to ignite. Velocity histories of the design modifications were compared to that of Round 25155. The T-bar at the inlet was the least effective. Both versions of the inlet screen showed some velocity variations, but round-to-round data were not consistent. The most consistent velocity data and drag reduction was observed with the configuration containing a T-bar in the combustion section.

The April 1985 series were fired to obtain additional performance data for the "T-bar in the Combustor" modification as well as to determine performance of three more energetic fuel combinations. The preliminary test data for this series is shown in Table A7. Figure A1 shows a comparison of the velocity histories of the modification with the T-bar in combustor and a non-thrusting model. Unfortunately, for this test series, the non-thrusting models had launch velocities around 4500 ft/sec while the thrusting models were launched at 4600 ft/sec. In spite of this initial velocity discrepancy, increased velocity was observed for the modified projectiles. Comparison of the velocity data for the inert model and the models with 115-HVAP fuel are shown in Figure A2. Velocity comparisons

for the 145-HVAP and 215-HVAP fuels are shown in Figures A3 and A4, respectively. These figures show that all the models fueled with more energetic compositions generated some thrust. Their velocity histories showed slope changes similar to the 75mm TGTR, but the break points were located between 1.6 and 2.0 seconds. On the other hand, the velocity histories of the models modified with a T-bar in their combustor sections did not show any slope change although they had increased velocity.

From the April tests, it was determined that changing the fuel composition was more effective than inserting various devices into the internal flowfield of the projectile. Of the three compositions tried in April, UTC fuel 25950 had the least amount of additional fuel oxidizer, Ammonium Perchlorate. It was hoped that some minor modification of this composition may generate thrust for a longer period than the observed 1.5-1.8 seconds or that it would generate a higher thrust for the same duration. The May 1985 "Hawk test" series was designed to determine the performance repeatability of the 215-HVAP fuel. The test results for this series are given in Table A8. A comparison of velocity histories showed large variations in the performance of this fuel composition in a 40mm SFRJ.

Range Tests

Tests conducted in October 1984 with Hawk support were inconclusive for defining the operation of a ramjet under the launch conditions using the 40mm L70 gun system. It was decided to obtain photographic data that could show some flow detail. This was accomplished in the TR facility with mosaic coverage.

In December 1984, three test rounds were fired to observe location of inlet shock and wake flowfield. Burning, if present, would be visible on the mosaic film. However, since the 40mm SFRJ has a pusher disk as part of its sabot system, it was essential to verify that the pusher would not enter the TR and damage the photographic instrumentation. Therefore, a four-round field test was fired to insure that the sabot components remained outside the TR. Preliminary results from this series, both the field and TR tests, are shown in Table A9. The models used for the field tests were designs with 406-HVAP fuel and never ignited.

The mosaic for the first test round showed an attached, oblique, leading-edge shock wave. The second projectile was a model made to simulate the actual design mass properties by using an aluminum ring in the combustor. This mosaic showed a detached, normal, leading-edge shock. The third round had a screen with round holes in the cowl. Hot gases from the burning fuel were visible on the shadowgraph plates at 150 feet from the gun. The mosaic also showed a detached, normal, leading-edge shock wave. This shock location is required for internal combustion, since the design requires subsonic internal flow.

The next series of TR tests were designed to determine aerodynamic coefficients of inert and active models at a particular flight Mach number. Table A10 is a summary of the preliminary results from this series. The Range tests consisted of six inert and 10 fueled models. Four of the inert rounds were modified with inlet screens. Two of the screens had large central holes, while the other two models had full-area screens. The remaining two inert rounds had standard configurations. All inert rounds had DC93-104 in place of fuel. Their mosaics showed attached, normal, leading-edge shocks.

One of the live rounds had 406 HVAP fuel and an inlet screen. Two rounds had 406 HVAP fuel and T-bar in the combustion area, while the remaining 6 models were of standard configuration with different fuel compositions. All the inert models had about 2.5 times more drag than the live rounds. However, the duration of this drag reduction was about 1.5 seconds for all live rounds.

Conclusions

The 40mm SFRJ projectile configuration, scaled from the 75mm version and without design modifications (e.g. T-bar in combustor and more energetic solid fuels) did not produce detectable thrust in flight tests. Design modifications, as described in this Appendix, achieved measureable thrust (i.e. drag reduction over the inert rounds) at comparable levels to the 75mm SFRJ. Changes to the solid fuel composition were found to be more effective than changes to internal geometry. However, the typical burn times (1.5 seconds) were significantly shorter (2.8-3.0 seconds) than those of the 75mm SFRJ. The reduction in burn time may be due in part to enhanced fuel regression caused by the higher spinrate of the 40mm SFRJ. As a result, the 40mm SFRJ design did not meet the original objective of increased velocity (or at least constant velocity) for 4000m of range.

Table A1. MATRIX FOR OCTOBER 1984 HAWK TEST SERIES

TYPE	NO.ROUNDS	HVAP	MODIFICATION
Warmer	3	406	Standard Design
Data Base	1	—	No Fuel, Empty Casing
Test Round	3	406	Screen with Round Holes
Test Round	3	406	Screen with Square Holes
Test Round	3	406	T-Bar in Inlet
Test Round	3	406	T-Bar in Combustor

Table A2. MATRIX FOR APRIL 1985 HAWK TEST SERIES

TYPE	NO.ROUNDS	UTC FUEL	HVAP	MODIFICATION
Warmer	3	—	406	Standard Design
Test Round	2	—	406	T-Bar in Combustor
Test Round	2	25950	215	Standard Design
Test Round	2	25048	145	Standard Design
Test Round	2	22032	115	Standard Design

Table A3. MATRIX FOR MAY 1985 HAWK TEST SERIES

TYPE	NO.ROUNDS	UTC FUEL	HVAP	MODIFICATION
Warmer	3	—	406	Standard Design
Test Round	5	25950	215	Standard Design

Table A4. MATRIX FOR DECEMBER 1984 MOSAIC TESTS

TYPE	NO.ROUNDS	HVAP	MODIFICATION
A- Field Test:			
Test Round	4	406	Standard Design
B- Mosaic Test:			
Check Round	1	406	Standard Design
Test Round	1	—	Aluminum Insert for Fuel
Test Round	1	406	Screen with Round Holes

Table A5. MATRIX FOR MAY 1985 RANGE TESTS

NO.ROUNDS	UTC FUEL	HVAP	MODIFICATION
1	—	406	Standard Design
2	DC93-104	Inert	Screen with Central Hole
2	DC93-104	Inert	Screen without Central Hole
2	DC93-104	Inert	Standard Design
2	25950	215	Standard Design
2	22032	115	Standard Design

Table A6. RESULTS FROM OCTOBER 1984 HAWK TEST SERIES

ROUND	SHELL S/N	UTC FUEL	HVAP	MODIFICATION	REMARKS
25154	123	—	406	Standard design	Warmer; poor Hawk data; poor smear data
25155	055	—	406	Standard design	Warmer; 14-sec Hawk data; no smear data
25156	195	—	406	Standard design	Warmer; 14-sec Hawk data; 1 smear operated
25157	—	No Fuel	—	Standard design	Data Base; good Hawk data; good smear data
25158	107	—	406	Screen with square holes	Data round; good Hawk data; good smear data; no visible ignition
25159	044	—	406	Screen with round holes	Data round; good Hawk data; good smear data; no visible ignition
25160	036 (5358B)	—	406	T-bar in cowl	Data round; good Hawk data; good smear data; burning at 90-ft
25161	024	—	406	T-bar in combustor	Data round; good Hawk data; good smear data; burning at 90-ft
25162	211	—	406	Screen with square holes	Data round; good Hawk data; good smear data; no visible ignition
25163	054	—	406	Screen with round holes	Data round; good Hawk data; good smear data; no visible ignition
25164	238	—	406	T-bar in cowl	Data round; good Hawk data; good smear data; ignition at 90-ft
25165	136 (5357B)	—	406	T-bar in combustor	Data round; good Hawk data; good smear data; ignition at 90-ft
25166	222 (5355B)	—	406	Screen with square holes	Data round; good Hawk data; good smear data; no visible ignition
Gun QE 235 mils (13.2 deg). Smear Camera Locations 12, 30, 60, 90 feet.					

Table A7. RESULTS FROM APRIL 1985 HAWK TEST SERIES

ROUND	SHELL S/N	UTC FUEL	HVAP	MODIFICATION	REMARKS
26020	173	—	406	Standard design	Warmer; good Hawk data
26021	199	—	406	Standard design	Warmer; 4.5-sec Hawk data
26022	179	—	406	Standard design	Warmer; 3.5-sec Hawk data
26023	043	—	406	T-bar in combustor	Data round; 5.5-sec Hawk data; indication of thrust
26024	118	—	406	T-bar in combustor	Data round; 5.1-sec Hawk data; indication of thrust
26025	075	22032	115	Standard design	Data round; 5.1-sec Hawk data; indication of thrust
26026	033	22032	115	Standard design	Data round; 5.1-sec Hawk data; indication of thrust
26027	045	25048	145	Standard design	Data round; 5.0-sec Hawk data; indication of thrust
26028	084	25048	145	Standard design	Data round; 5.0-sec Hawk data; indication of thrust
26029	168	25950	215	Standard design	Data round; 5.0-sec Hawk data; indication of thrust
Gun QE 235 mils (13.2 deg). Smear Camera Locations 12, 30, 60, 90 feet.					

Table A8. RESULTS FROM MAY 1985 HAWK TEST SERIES

ROUND	SHELL S/N	UTC FUEL	HVAP	MODIFICATION	REMARKS
26197	132	—	406	Standard design	Warmer; good Hawk data; good smear data
26198	237	25950	215	Standard design	Data round; good Hawk data; good smear data; ignition at 90-ft (Hawk recorder capstan broke)
26199	178	—	406	Standard design	Warmer; good Hawk data; good smear data
26200	046	25950	215	Standard design	Data round; good Hawk data; good smear data; ignition at 90-ft
26201	218	25950	215	Standard design	Data round; good Hawk data; good smear data; ignition at 90-ft
26202	151	25950	215	Standard design	Data round; good Hawk data; good smear data; ignition at 90-ft
26203	189	25950	215	Standard design	Data round; good Hawk data; good smear data; ignition at 90-ft; indication of yawing at 30 and 60-ft
26204	074	25950	215	Standard design	Data round; good Hawk data; good smear data; ignition at 90-ft
Gun QE 90 mils (5.0 deg). Smear Camera Locations 12, 30, 60, 90 feet.					

Table A9. RESULTS FROM MAY 1985 HAWK TEST SERIES

ROUND	SHELL S/N	HVAP	MODIFICATION	REMARKS
FIELD TESTS *				
25495	180	406	Standard Design	Target at 70-ft Pusher impacted 1 caliber from model
25496	214	406	Standard Design	Target at 100-ft Pusher impacted 4 calibers from model
25497	190	406	Standard Design	Target at 100-ft Pusher impacted 13 calibers from model
25498	210	406	Standard Design	Target at 100-ft Pusher impacted 6 calibers from model
MOSAIC TESTS **				
25512	187	406	Standard Design	Check round; good shadowgraphs; good mosaic; attached shock
25513	219	—	Aluminum Insert to Simulate Fuel	Data round; good shadowgraphs; good mosaic; detached shock
25514	183	406	Screen with Round Hole	Data round; good shadowgraphs; good mosaic; detached shock
* Gun QE 0 mils, Smear Camera Locations 12, 30, 60 feet.				
** Gun QE 0 mils, Located 150-ft from Station 1-1. Mosaic Located 400-ft from Gun.				

Table A10. RESULTS FROM MAY 1985 HAWK TEST SERIES

ROUND	SHELL S/N	BRL NO	UTC FUEL	HVAP	MODIFICATIONS	REMARKS
26205	192	—	—	406	Standard Design	Spotty shadowgraphs; burning; good mosaic; attached shock
26206	112	5401B	DC93-104	Inert	Screen with Central Hole	Good shadowgraphs; good mosaic; attached shock
26216	111	5402B	DC93-104	Inert	Screen with Central Hole	Good shadowgraphs; good mosaic; attached shock
26217	085	5403B	DC93-104	Inert	Screen without Central Hole	Good shadowgraphs; good mosaic; attached shock
26218	068	5404B	DC93-104	Inert	Screen without Central Hole	Good shadowgraphs; good mosaic; attached shock
26219	100	5406B	DC93-104	Inert	Standard Design	Good shadowgraphs; poor mosaic; attached shock
26220	053	5405B	DC93-104	Inert	Standard Design	Good shadowgraphs; good mosaic; attached shock; nose collapsed (?)
26221	125	5385B	25950	215	Standard Design	Spotty shadowgraphs; good mosaic; detached shock
26222	097	5384B	22032	115	Standard Design	Spotty shadowgraphs; good mosaic; detached shock
Gun QE 0 mils, Located 150-ft from Station 1-1. Smear Cameras at 59 and 78 feet. Mosaic Located 400 feet from Gun.						

COMPARISON BASE VS T-BAR

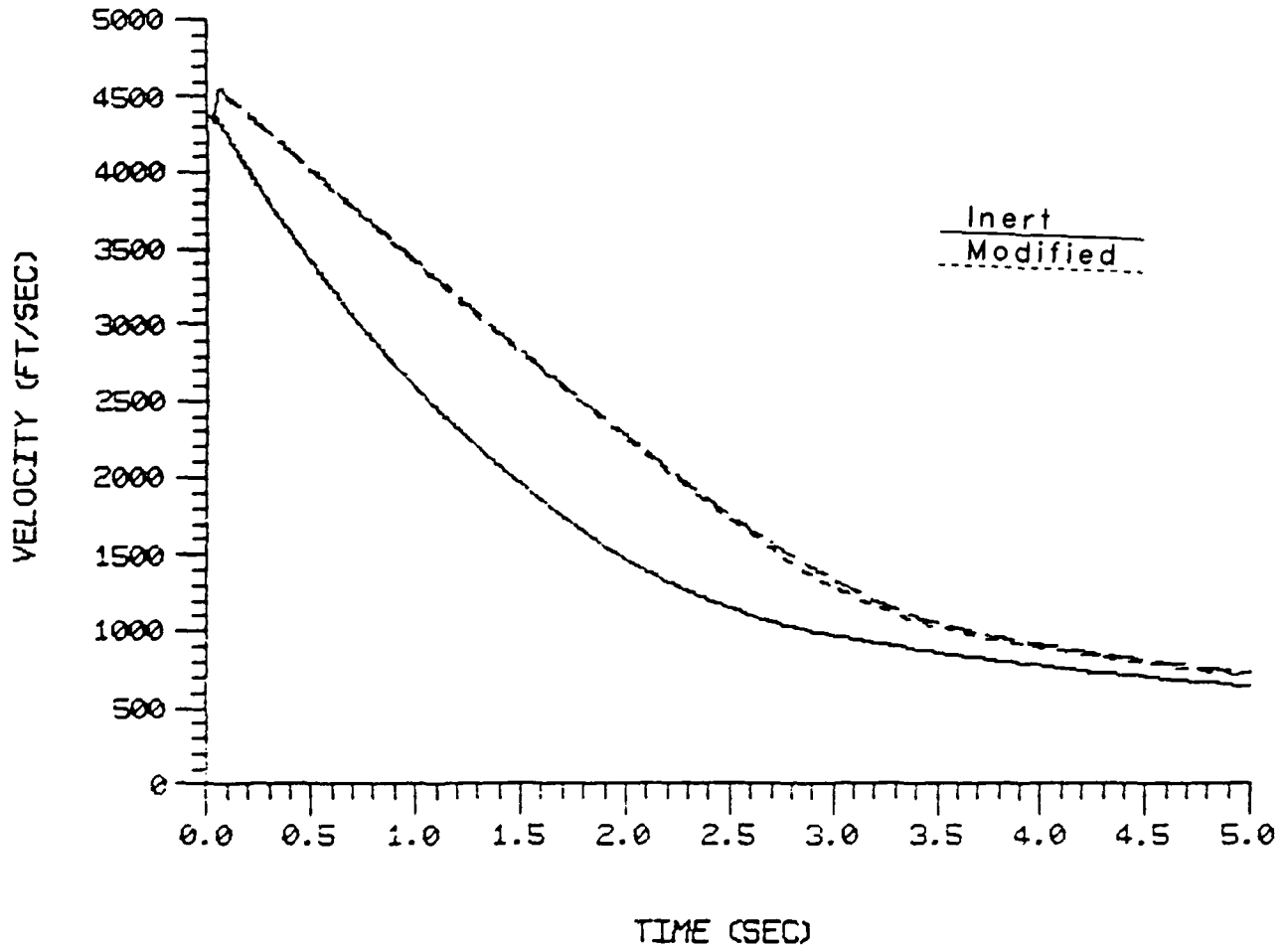


Figure A1. Velocity Comparison for Inert and Modified (T-Bar in Combustor) Models - April 1985 Series

COMPARISON BASE VS HVAP=115

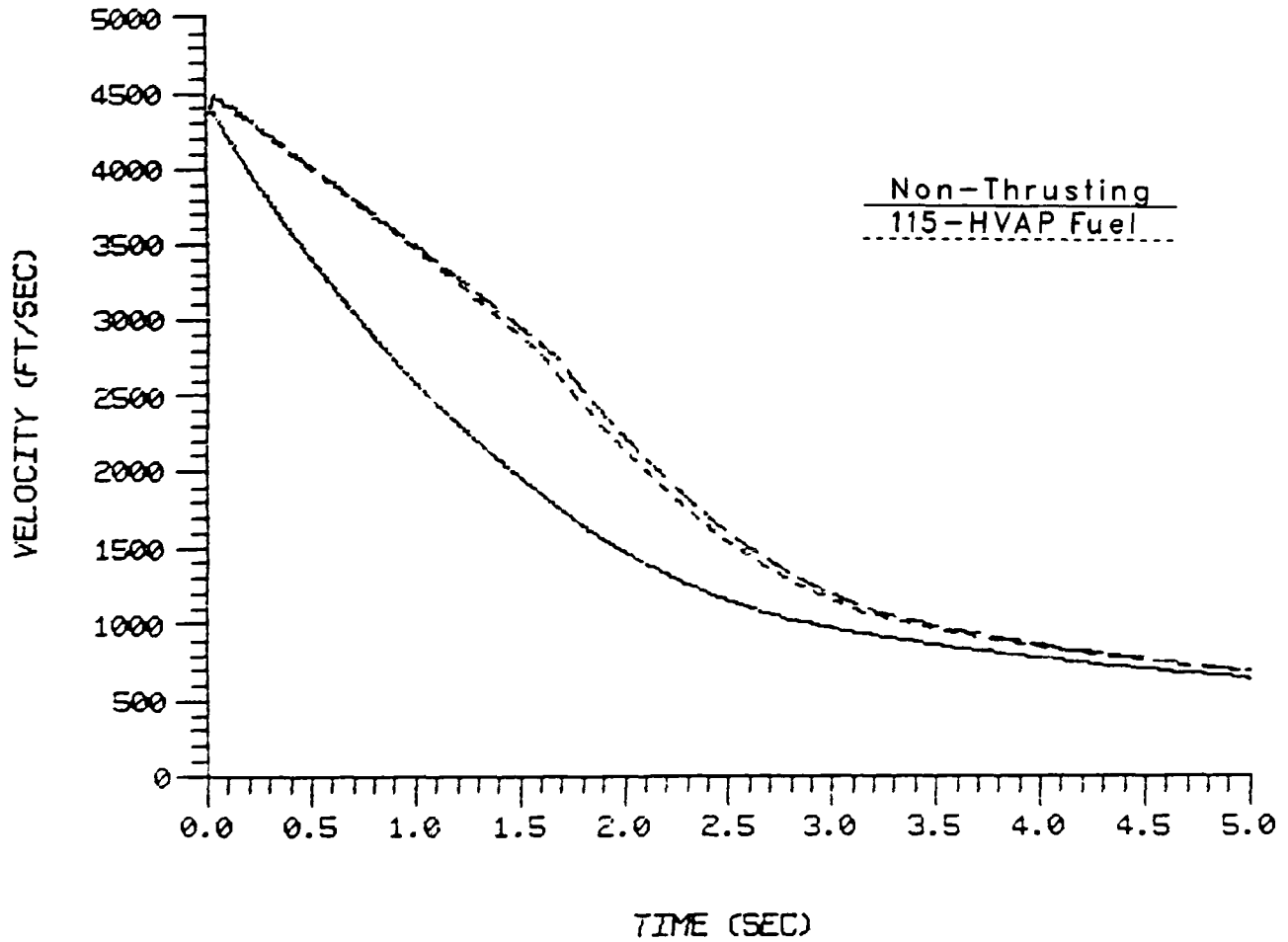


Figure A2. Velocity Comparison for Non-Thrusting and 115-HVAP Fuel Models - April 1985 Series

COMPARISON BASE VS HVAP=145

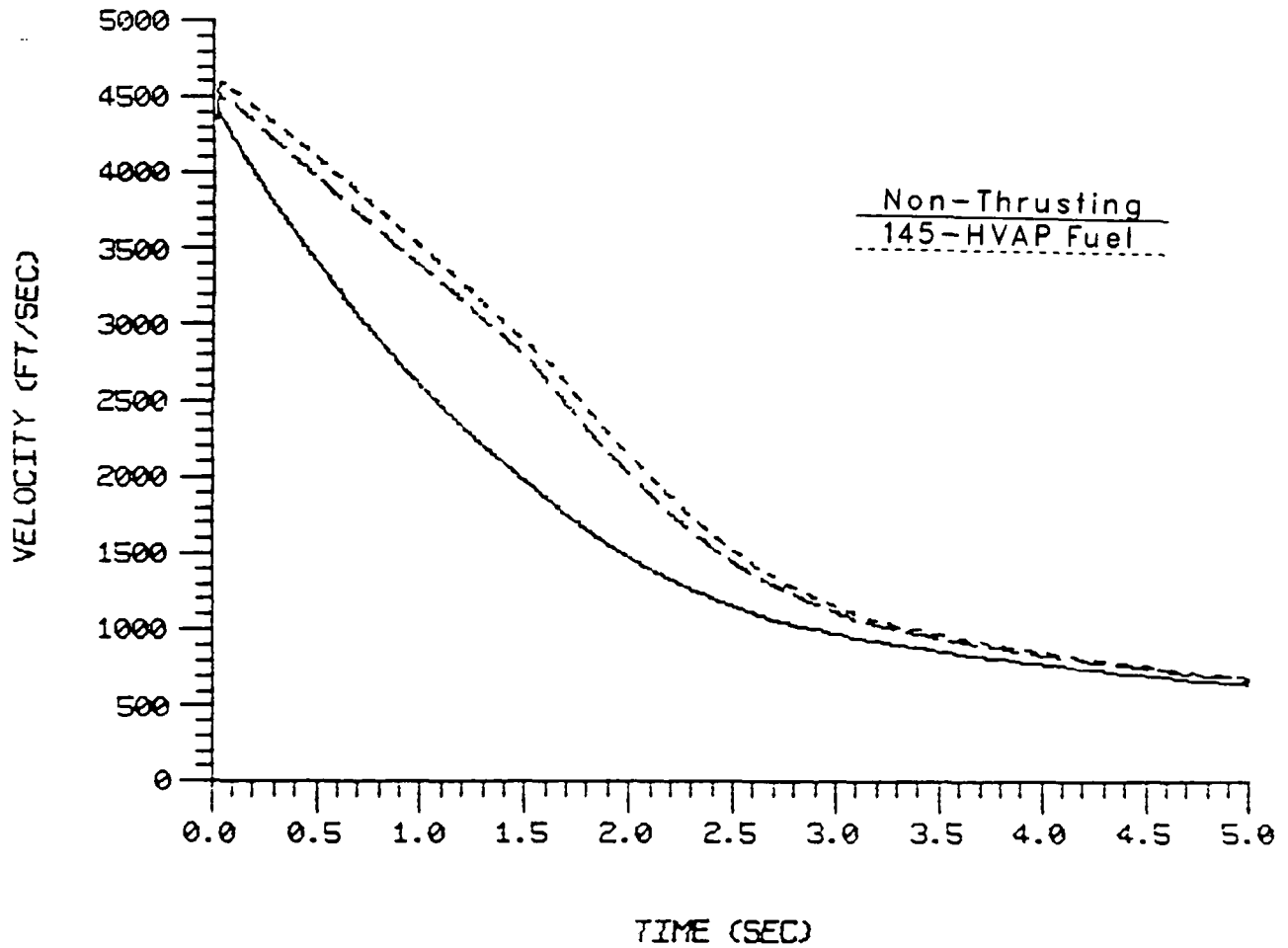


Figure A3. Velocity Comparison for Non-Thrusting and 145-HVAP Fuel Models - April 1985 Series

COMPARISON BASE VS HVAP=215

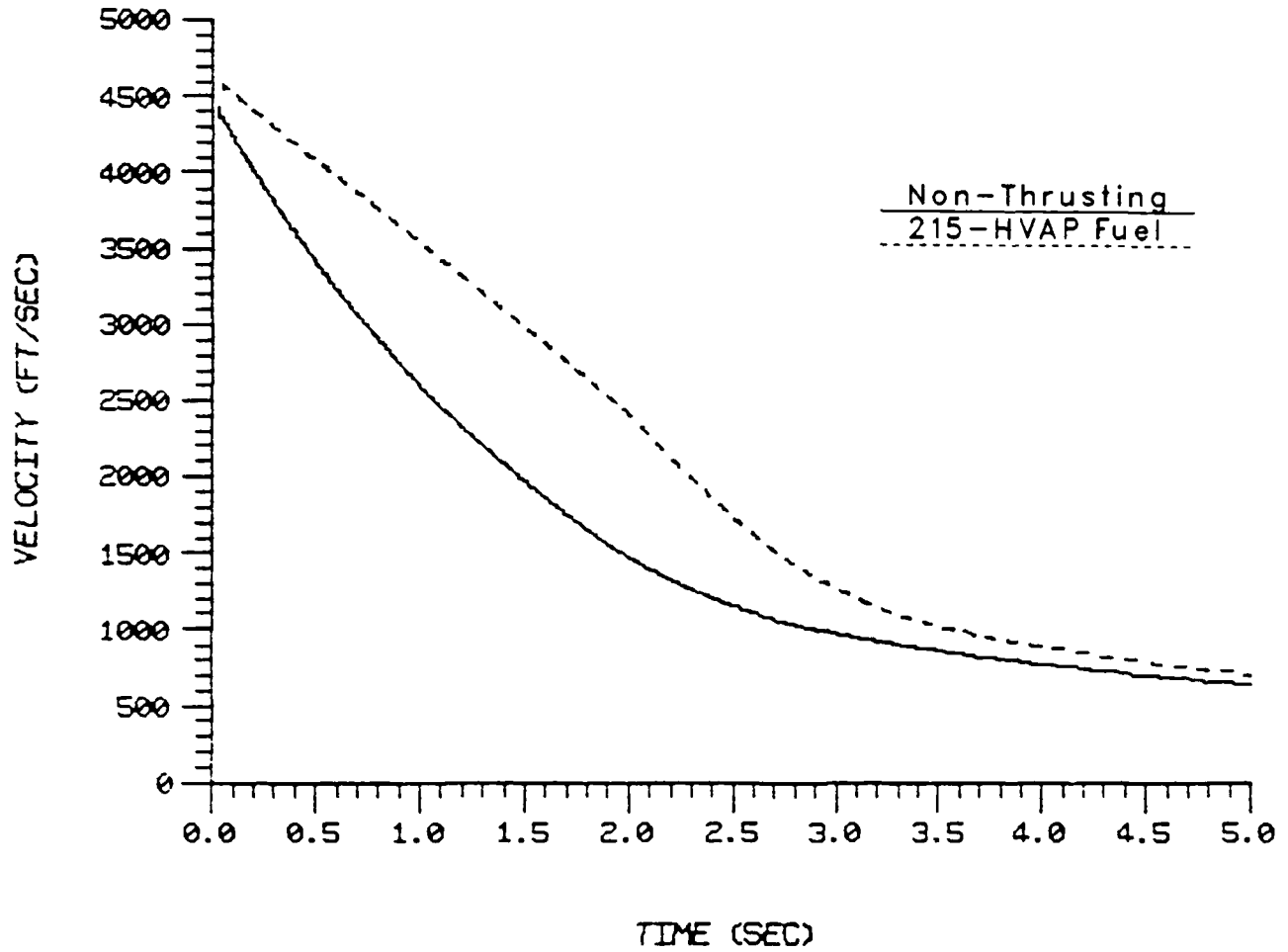


Figure A4. Velocity Comparison for Non-Thrusting and 215-HVAP Fuel Models - April 1985 Series

DISTRIBUTION LIST

<u>No. of Copies</u>	<u>Organization</u>	<u>No. of Copies</u>	<u>Organization</u>
12	Administrator Defense Technical Info Center ATTN: DTIC-DDA Cameron Station Alexandria, VA 22304-6145	1	Director Benet Weapons Laboratory Armament RD&E Center US Army AMCCOM ATTN: SMCAR-LCB-TL Watervliet, NY 12189-4050
1	HQDA (SARD-TR) Washington, DC 20310-0001	1	Commander US Army Armament, Munitions and Chemical Command ATTN: SMCAR-ESP-L Rock Island, IL 61299-5000
1	Commander US Army Materiel Command ATTN: AMCDRA-ST 5001 Eisenhower Avenue Alexandria, VA 22333-0001	1	Commander US Army Aviation Systems Command ATTN: AMSAV-DACL 4300 Goodfellow Blvd. St. Louis, MO 63120-1798
1	Commander US Army Laboratory Command ATTN: AMSLC-DL Adelphi, MD 20783-1145	1	Director US Army Aviation Research and Technology Activity Anes Research Center Moffett Field, CA 94035-1099
2	Commander Armament RD&E Center US Army AMCCOM ATTN: SMCAR-MSI Picatinny Arsenal, NJ 07806-5000		
2	Commander Armament RD&E Center US Army AMCCOM ATTN: SMCAR-TDC Picatinny Arsenal, NJ 07806-5000		
1	Commander Armament RD&E Center US Army AMCCOM ATTN: SMCAR-AER-A (R. Kline) Picatinny Arsenal, NJ 07806-5000	1	Commander US Army Missile Command ATTN: AMSMI-AS Redstone Arsenal, AL 35898-5010
2	Commander Armament RD&E Center US Army AMCCOM ATTN: SMCAR-FSP-A (F. Scarbo) (J. Bera) Picatinny Arsenal, NJ 07806-5000	1	Commander US Army Tank Automotive Command ATTN: ASQNC-TAC-DI (Technical Library) Warren, MI 48397-5000

DISTRIBUTION LIST

<u>No. of Copies</u>	<u>Organization</u>	<u>No. of Copies</u>	<u>Organization</u>
1	Director US Army TRADOC Analysis Command ATTN: ATAA-SL White Sands Missile Range NM 88002-5502	1	Director National Aeronautics and Space Administration Langley Research Center ATTN: Technical Library Langley Station Hampton, VA 23365
1	Commandant US Army Infantry School ATTN: ATSH-CD-CSO-OR Fort Benning, GA 31905-5660	1	Director National Aeronautics and Space Administration Marshall Space Flight Center ATTN: Dr. W.W. Fowlis Huntsville, AL 35812
1	AFWL/SUL Kirtland AFB, NM 87117-5800	1	Director National Aeronautics and Space Administration Ames Research Center ATTN: Dr. J. Steger Moffett Field, CA 94035
1	Air Force Armament Laboratory ATTN: AFATL/DLODL Eglin AFB, FL 32542-5000	1	Aerospace Corporation Aero-Engineering Subdivision ATTN: Walter F. Reddall El Segundo, CA 90245
1	Commander Naval Surface Weapons Center ATTN: Dr. W. Yanta Aerodynamics Branch K-24, Bldg. 402-12 White Oak Laboratory Silver Spring, MD 20910	1	Calspan Corporation ATTN: W. Rae P.O. Box 400 Buffalo, NY 14225
1	Commander Defense Advanced Research Projects Agency ATTN: MAJ R. Lundberg 1400 Wilson Blvd. Arlington, VA 22209	1	Hughes Aircraft ATTN: Dr. John McIntyre Mail Code S41/B323 P.O. Box 92919 Los Angeles, CA 90009
1	Director Lawrence Livermore National Laboratory ATTN: Mail Code L-35 (Mr. T. Morgan) P.O. Box 808 Livermore, CA 94550	1	Interferometrics, Inc. ATTN: Mr. R.F. L'Arriva 8150 Leesburg Pike Vienna, VA 22180
2	Director Sandia National Laboratories ATTN: Dr. W. Oberkampf Dr. W.P. Wolfe Division 1636 Albuquerque, NM 87185	2	United Technologies Corporation Chemical Systems Division ATTN: Dr. R.O. MacLaren Mr. A.L. Holzman 600 Metcalf Road, P.O. Box 50015 San Jose, CA 95150-0015

DISTRIBUTION LIST

<u>No. of Copies</u>	<u>Organization</u>	<u>No. of Copies</u>	<u>Organization</u>
3	Rockwell International Science Center ATTN: Dr. V. Shankar Dr. S. Chakravarthy Dr. U. Goldberg 1049 Camino Dos Rios P.O. Box 1085 Thousand Oaks, CA 91360	1	University of Colorado Department of Astro-Geophysics ATTN: E.R. Benton Boulder, CO 80302
1	Arizona State University Department of Mechanical and Energy Systems Engineering ATTN: Dr. G.P. Neitzel Tempe, AZ 85281	1	University of Delaware Spencer Laboratory Department of Mechanical Engineering ATTN: Prof. Leonard W. Schwartz Newark, DE 19716
1	Director Johns Hopkins University Applied Physics Laboratory ATTN: Dr. Fred Billig Johns Hopkins Road Laurel, MD 20707	2	University of Maryland ATTN: W. Melnik J.D. Anderson College Park, MD 20740
1	Massachusetts Institute of Technology ATTN: H. Greenspan 77 Massachusetts Avenue Cambridge, MA 02139	1	University of Maryland Baltimore County Department of Mathematics ATTN: Dr. Y.M. Lynn 5401 Wilkens Avenue Baltimore, MD 21228
1	North Carolina State University Mechanical and Aerospace Engineering Department ATTN: F.F. DeJarnette Raleigh, NC 27607		<u>Aberdeen Proving Ground</u> Director, USAMSAA ATTN: AMXSY-D AMXSY-MP, H. Cohen
1	Northwestern University Department of Engineering Science and Applied Mathematics ATTN: Dr. S.H. Davis Evanston, IL 60201		Commander, USATECOM ATTN: AMSTE-TO-F
1	Renssalaer Polytechnic Institute Department of Math Sciences Troy, NY 12181		Commander, CRDEC, AMCCOM ATTN: SMCCR-RSP-A M.C. Miller D. Olsen SMCCR-MJ W. Dee C. Hughes D. Bromley SMCCR-SPS-IL
1	University of California - Davis ATTN: Dr. Harry A. Dwyer Davis, CA 95616		

USER EVALUATION SHEET/CHANGE OF ADDRESS

This laboratory undertakes a continuing effort to improve the quality of the reports it publishes. Your comments/answers below will aid us in our efforts.

- 1. Does this report satisfy a need? (Comment on purpose, related project, or other area of interest for which the report will be used.) _____

- 2. How, specifically, is the report being used? (Information source, design data, procedure, source of ideas, etc.) _____

- 3. Has the information in this report led to any quantitative savings as far as man-hours or dollars saved, operating costs avoided, or efficiencies achieved, etc? If so, please elaborate. _____

- 4. General Comments. What do you think should be changed to improve future reports? (Indicate changes to organization, technical content, format, etc.) _____

BRL Report Number _____ Division Symbol _____

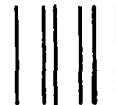
Check here if desire to be removed from distribution list. _____

Check here for address change. _____

Current address: Organization _____
Address _____

-----FOLD AND TAPE CLOSED-----

Director
U.S. Army Ballistic Research Laboratory
ATTN: SLCBR-DD-T (NEI)
Aberdeen Proving Ground, MD 21005-5066



NO POSTAGE
NECESSARY
IF MAILED
IN THE
UNITED STATES

OFFICIAL BUSINESS
PENALTY FOR PRIVATE USE \$300

BUSINESS REPLY LABEL
FIRST CLASS PERMIT NO. 12062 WASHINGTON D. C.

POSTAGE WILL BE PAID BY DEPARTMENT OF THE ARMY



Director
U.S. Army Ballistic Research Laboratory
ATTN: SLCBR-DD-T (NEI)
Aberdeen Proving Ground, MD 21005-9989

SUPPLEMENTARY

INFORMATION

AD-A 206536

May 1989 Errata

**“Comparison of Computational Analysis with Flight Tests
of a 40MM Solid-Fuel Ramjet Projectile,” BRL-TR-2983,
M.J. Nusca and V. Oskay, March 1989.**

Four (4) citations are to be inserted after the first sentence of Section II. Background, i.e. “During the early 1980’s, U.S. Army Chemical Research Development and Engineering Center (CRDEC) began development of a 40mm Solid-Fuel Ramjet (SFRJ) projectile as a possible air defense round.”

Mermagen, W.H. and Olson, D., “Initial Test Firings of a Solid Fuel Ramjet Tubular Projectile,” ARBRL-MR-03212, U.S. Army Ballistic Research Laboratory, Aberdeen Proving Ground, MD, November 1982, (AD B069824).

Mermagen, W.H. and Olson, D., “Demonstration Test Firings of a Solid Fuel Ramjet Tubular Projectile,” ARBRL-MR-03213, U.S. Army Ballistic Research Laboratory, Aberdeen Proving Ground, MD, November 1982, (AD B069823).

Miller, M.C. and Olson, D., “Solid Fuel Ramjet Tubular Projectile,” ARCSL-TR-83041, U.S. Army Chemical Systems Laboratory, Aberdeen Proving Ground, MD, June 1983, (AD B078019).

MacLaren R.O. and Holzman, A.L., “40mm Solid Fuel Ramjet Tubular Projectile,” CRDEC-CR-87067, U.S. Army Chemical Research Development and Engineering Center, Aberdeen Proving Ground, MD, April 1987, (AD B111645).